IEEE Access
Multidisciplinary ⁝ Rapid Review ⁝ Open Access Journal

Received January 18, 2018, accepted March 11, 2018, date of current version July 12, 2018.

Digital Object Identifier 10.1109/ACCESS.2018.2817648

Path Planning of UAVs Based on Collision Probability and Kalman Filter

ZHENYU WU, JINHUAN LI, JIAMING ZUO, AND SHENGMING LI
School of Innovation and Entrepreneurship, Dalian University of Technology, Dalian 116024, China
Corresponding author: Jinhuan Li (770796776@qq.com)

ABSTRACT For clusters of UAVs, the scale and density of the cluster determine its ability to solve the task. With the increasing density of aerial vehicles, effectively planning a reasonable flight path and avoiding conflicts among flight paths have become key problems for UAV clusters. The traditional control method is to detect potential conflicts through radar monitoring or location reporting in the air and to then change the flight path, including the height, heading, and speed, through manual instruction. To solve the problem of path conflicts for UAV clusters, a method for calculating the collision probabilities of UAVs is established under the constraints of mission space and the number of UAVs. In cluster flight mode, automatic tracking and prediction of UAV cluster tracks are implemented to avoid path conflicts in clusters. In addition, to address the inconsistency problem because of noise caused by the state information of multi UAV communication under a dynamic environment, a state estimation method is proposed based on the Kalman algorithm. To achieve aircraft track planning, cluster state prediction and collision probability are eventually calculated to avoid the clusters of formation UAVs conflicting on paths during flight. Finally, the simulation results verify the validity and effectiveness of the proposed method in multi UAV formation flight planning.

INDEX TERMS UAVs, collision probability, trajectory conflict, state estimation.

I. INTRODUCTION

Collision is a very important problem in the movement of objects. In the course of motion and path planning, collisions are a factor that has to be considered; therefore, it is necessary to calculate the collision probability [1]–[5].

The density of a multi UAV cluster determines the scale of the task it can solve. With the increasing cluster density, effectively planning flight paths of aircraft and avoiding conflicts among the aircraft flight paths have become key problems in multi UAV path planning. Multi UAV clusters must maintain a safe distance and altitude difference in formation flight or target tracking, but the interval distances between aircrafts and the height differences cannot remain constant due to the influences of various factors. If the flight paths are not well planned, collisions could easily occur between UAVs. Therefore, collision avoidance in cluster flight has become a field worthy of study and concern.

If the relative speed of two targets is fast when they are approaching, the relative motion of the two targets can be considered linear relative motion, in which the motions of two targets are assumed to be linear during the approaching period and velocity uncertainty is neglected. Therefore, the position error ellipsoid remains the same during the approaching period. The position error can be described by the covariance matrix, and the covariance matrixes of the two targets are not related. A collision is assumed to occur when the distance between the aircraft is less than the equivalent radius (or the radius given), so the collision probability is defined as the probability when the distance between two targets is less than the sum of their equivalent radius.

According to this assumption, the relative position vector and the relative velocity vector are vertical at the closest position, and the two targets are in the planes that are perpendicular to the plane of the relative velocity, which is defined as the encounter plane. Because the covariance matrixes of two targets are uncorrelated, the position error of the two targets can be combined as a joint ellipsoid error, and the equivalent radius can be combined as a joint sphere, which can then become a joint error ellipse and a joint circular domain, respectively, after projecting to the encounter plane. Taking the encounter plane as the datum plane and taking the relative velocity vector as the reference direction, we can obtain the encounter coordinate system. Then, the collision probability problem can be transformed into the calculation of the integral of a two-dimensional probability density function (PDF) in the circle region through error projection.

However, it is difficult to obtain an analytical solution of the double integral. Therefore, finding an integral method that has high accuracy and high speed is the key to calculating the collision probability.

Foster transforms polar coordinates in the encounter plane, divides the double integral of Descartes coordinates into two integrals about the polar coordinates, and then calculates them according to the size with a certain step [6]. Patera, from the company Aerospace, proposed an equivalent numerical integration model that divides the two-dimensional area into one-dimensional curve integrals around the perimeter of the area with coordinate rotation and polar coordinate transformation; this method contains only an exponential function. This method does not need to assume that the two targets are spherical, and it can calculate the probability of any target of irregular shape [7]–[10]. Alfano, from the Center for Space and Innovation, deduced a series expression expressed by an error function and exponential function and obtained the expressions of the minimum series terms [11]–[14]. Based on typical actual proximity and error parameters, Chan, from the company Aerospace, transformed the two-dimensional Gauss distribution of PDF into a Rician distribution of PDF and deduced the approximate analytical expressions of the double integral by using the concept of equivalent area [15]–[18]. These methods differ in the methods used to solve the double integral in the encounter plane. The methods of Foster, Patera and Alfano are essentially numerical methods, while the method of Chan is an analytical method. Alfano uses different parameter examples to compare the above methods [19].

The method of Chan is the fastest computing method and has the strictest restrictive parameter, so it is suitable for fast calculation of collision probability. The Patera method has high accuracy, which is suitable for irregular object shapes, and Alfano's method can determine the number of terms in a series according to different calculation examples. Both of these methods are suitable for accurate calculation of the collision probability in maneuvering decisions. Foster's method is the slowest but can be accelerated by increasing the step size. The conjunction data message (CDM) of the Consultative Committee for Space Data Systems (CCSDS) recommends standards for the SEC information exchange format to contribute to a general framework and to provide a common foundation. There are four options for calculating collision probability, namely, Foster's method, Chan's method, Patera's method and Alfano's method [20]. The collision probability calculation under vehicle information exchange is analyzed in [21].

According to the previous study, we found that UAVs have the following problems: the contradiction between cluster density and collision avoidance, the interference of communication noise in action consistency, and the path planning of UAVs. In this paper, a time-space protection model based on the gravitational potential field and Kalman state estimation algorithm is designed to solve the problem.

In general, the first chapter in this paper introduces the overall study, while the calculation method of the UAV collision probability and analysis are introduced in detail in the second, third and fourth chapters. The simulation experiments in the fifth chapter verify the filtering effect of the Kalman filtering method for communication noise in UAV collision probability. The sixth chapter summarizes this article.

II. CALCULATION METHOD OF MULTI UAV COLLISION PROBABILITY

In three-dimensional space, calculating the collision probability is the basic problem of UAV collision detection and effective avoidance. The collision probability of UAVs is related to many parameters, and there are many calculation methods. In this paper, the collision probability of UAV in formation flying is analyzed by means of the probability calculation and collision avoidance method of satellites or other spacecraft. following the collision probability analysis in satellites, when analyzing the collision problems of UAVs flying in formation, we assume that the UAVs move linearly. Therefore, the two UAVs move in uniform linear motion, and their speed can be measured, so that the location error ellipsoids maintain unchanged when they meet. We assume that the two groups of UAVs will collide or have already collided when the distance between the two groups of UAVs is smaller than their actual radius. The collision probability refers to the probability that the distance between two groups of UAVs is less than the sum of their radii. The collision probability is not only a valid standard for reducing and avoiding UAV collisions and showing the risk coefficient when UAVs are meeting but also an important basis for avoiding obstacles.

A. THE HYPOTHESIS OF THE COLLISION PROBABILITY ALGORITHM

The collision probability of formation UAVs is usually determined by the covariance matrixes of the position errors, shape and track of the aircraft. Therefore, to calculate the collision probability between UAVs, we must know the following two sets of data:

(1) the position vector of the UAVs during the encounter and

(2) the position error vector of the UAVs during the encounter.

The position vector in (1) is the amount of real-time UAV flight and can be calculated by an airborne computer; the UAV position error vector data in (2) is usually obtained by prediction error, which is considered to be produced in the presentation of this paper. The existence of position errors causes "misunderstandings" of position to other UAVs. It is necessary to evaluate the risk when UAVs meet according to the size of the collision probability. Then, based on the UAV collision probability, the UAVs can safely avoid collision. Therefore, the collision probability exists because of the position error. In addition, the position error vector in (2) must also be predicted and analyzed.

Therefore, to analyze the problem and to facilitate data processing, in this paper, we assume the following conditions:

(1) The position error satisfies the Gauss distribution, which is equal to a constant.

(2) When UAVs meet, because the time is very short, the process is regarded as static, and the motion of the UAVs is assumed to have a linear velocity and zero error.

(3) The UAV shape is considered the smallest enveloping sphere that can completely envelop the aircraft. In the calculation of collision, a combined envelope ball contains reference UAV and the other UAV.

(4) The covariance matrixes of the UAV positions are not related. Thus, for the formation flight of the UAV, the position of the covariance matrix of reference UAV is C_r, the position of the covariance matrix of the other UAV is C_f, and the relative position of the covariance matrix (joint ellipsoid error covariance matrix) of the two UAVs is $C_e = C_r + C_f$.

In addition, the random factors that may occur in the moment are accounted for in the reference UAV; that is, the reference UAV is the center of the error ellipsoid.

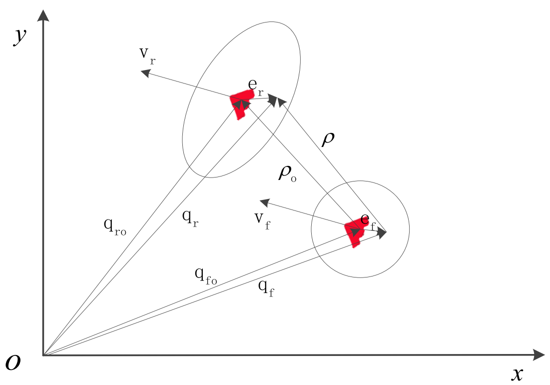

FIGURE 1. The geometric relationship diagram of the location of the UAVs.

B. DEFINITION OF THE COORDINATE SYSTEM

As shown in Figure 1, the collision probability is the probability of the distance between the two UAVs being less than the sum of the envelope radii. The distance between the two UAVs is $\rho = |q_r\text{-}q_f|$, where q_r and q_f are the position vectors of the reference UAV and the other UAV, respectively. The random error vectors of the two UAVs are e_r and e_f. Then, $q_r = q_{r0} + e_r$, and $q_f = q_{f0} + e_f$. Set the initial time $t_0 = 0$. Then, the actual relative position vector of the two UAVs at time t is

$$\begin{aligned}\rho(\mathrm{t}) &= \mathrm{q_r(t)} - \mathrm{q_f(t)} = (\mathrm{q_r} + \mathrm{v_r}\cdot \mathrm{t}) - (\mathrm{q_f} + \mathrm{v_f}\cdot \mathrm{t}) \\ &= (\mathrm{q_{ro}} + \mathrm{e_r} + \mathrm{v_r}\cdot \mathrm{t}) - (\mathrm{q_{fo}} + \mathrm{e_f} + \mathrm{v_f}\cdot \mathrm{t}) \\ &= \rho_\mathrm{o} + \mathrm{e_{ef}} + \mathrm{v_{rf}}\cdot \mathrm{t} = \rho + \mathrm{v_{rf}}\cdot \mathrm{t} \end{aligned} \tag{1}$$

where v_r and v_f are the speeds of the reference UAV and random UAV, respectively; e_r and e_f are the random error vectors of the reference UAV and random UAV, respectively; q_{r0} and $q_{\mathrm{f}0}$ are the central vectors of the reference UAV and random UAV, respectively; ρ_0 is the relative center vector, e_{ef} is the relative random error vector; and v_{rf} is the relative velocity vector.

The minimum value of the relative position vector $\rho(t)$ is equivalent to the minimum value of $\rho^2(t)$:

$$\rho^2(\mathrm{t}) = \rho(\mathrm{t}) \cdot \rho(\mathrm{t}) \tag{2}$$

Taking the derivative of the above equation gives

$$\begin{aligned}\frac{d}{dt}\left[\rho^2(t)\right] &= \frac{d}{dt}\left[(\rho + v_{rf}\times t)\times(\rho + v_{rf}\times t)\right] \\ &= 2\rho v_{rf} + 2v_{rf}^2 t^2 \end{aligned} \tag{3}$$

To obtain the minimum $\frac{d}{dt}[\rho^2(\mathrm{t})] = 0$, the following equation is used:

$$2\rho v_{rf} + 2v_{rf}^2 t^2 = 0 \tag{4}$$

According to equation (4), because $\mathrm{V_{rf}} \neq 0$, the time at which the minimum distance occurs between the two UAVs is

$$t_{\min-\mathrm{d}} = -\frac{\rho\cdot v_{rf}}{v_{rf}\cdot v_{rf}} \tag{5}$$

When $t = t_{\min-\mathrm{d}}$,

$$\rho(t_{\min-\mathrm{d}}) = \rho + \mathrm{v_{rf}}\cdot t_{\min-\mathrm{d}} = \rho + \mathrm{v_{rf}}\cdot[-\frac{\rho\cdot v_{rf}}{v_{rf}\cdot v_{rf}}] \tag{6}$$

Multiplying both sides of the above equation by $\mathrm{V_{rf}}$ gives

$$\rho(t_{\min-\mathrm{d}})\cdot \mathrm{v_{rf}} = \rho\cdot \mathrm{v_{rf}} - \rho\cdot \mathrm{v_{rf}} = 0. \tag{7}$$

According to the above equation, when the actual distance between the two UAVs is at its minimum, $\rho(\mathrm{t_{min-d}})$ is perpendicular to v_{rf}. At this point, the two sets of UAVs are in the vertical plane of the relative velocity of the two UAVs; this plane is called the encounter plane. Therefore, the position information of the two UAVs is projected onto the encounter plane, and the two-dimensional method is used to solve the three-dimensional problem. The collision problem of two UAVs in space can be analyzed by the plane method.

As shown in Figure 2, based on the definition of the encounter plane, the encounter coordinates can be defined. The centroid of the reference UAV is the origin O, the X axis is along the relative coordinate position vector of the two UAVs, the Y axis is along the relative velocity vector, and Z axis is perpendicular to this plane, following the right hand rule. The X-Y plane is the encounter plane.

III. CALCULATION METHOD OF COLLISION PROBABILITY

By defining the coordinate system centered on the reference UAV, the calculation of the collision probability can be transformed into an integral of the probability density function of the equivalent region.

In the encounter coordinate system, the relative position error of the UAV flight satisfies the Gauss distribution, and the probability density function of the three-dimensional normal distribution is

$$f(\mathrm{r}) = \frac{1}{(2\pi)^{\frac{3}{2}}|C_e|^{\frac{1}{2}}} e^{(-\frac{1}{2}r^T C_e^{-1} r)} \tag{8}$$

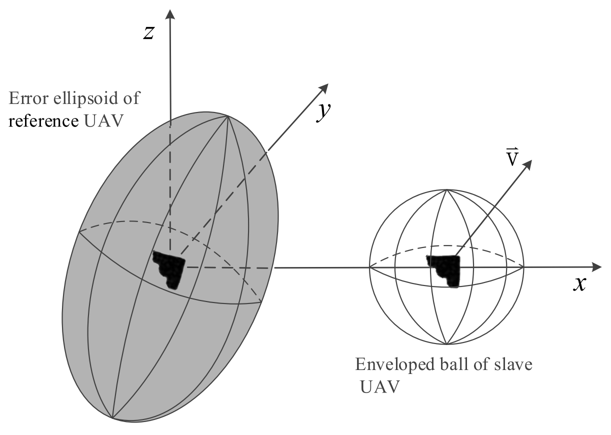

FIGURE 2. The UAV encounter coordinate schematic diagram.

where $|C_e|$ is the determinant of the covariance matrix of the relative position error of two UAVs and the physical meaning of $f(r)$ is the probability function when the distance between the origin and the reference UAV is r at time t.

Therefore, the probability of collision between two UAVs at time t is

$$P = \iiint_V f(r)\, dxdydz \tag{9}$$

where V is the volume of the two envelopes in three-dimensional coordinate space within the swept volume of a cylinder, as shown in Fig. 3.

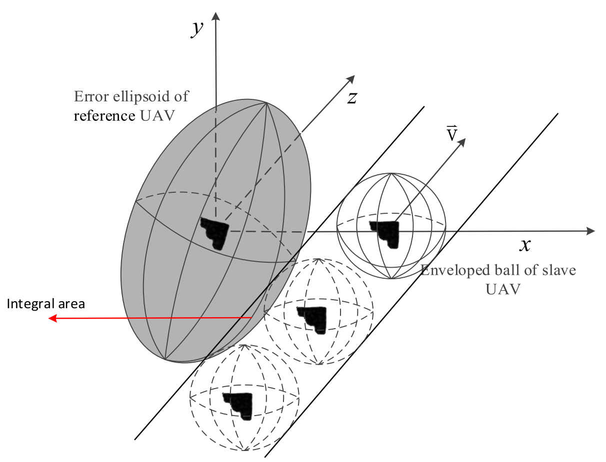

FIGURE 3. Integration region diagram.

In the entire flight of the UAVs, the UAV relative velocity and position error matrix change over time. However, because the encounter occurs within a very short period of time, this variation is very small. The changes in the relative velocity vector on the Z axis can be neglected, so we can neglect the time problem in the calculation, which means changing the problem of when the UAVs collide into the problem of whether a collision has occurred.

The variance of the relative random error vector e_{ef} of two UAVs is the matrix $Var(e_{ef})$, and it should be the diagonal matrix:

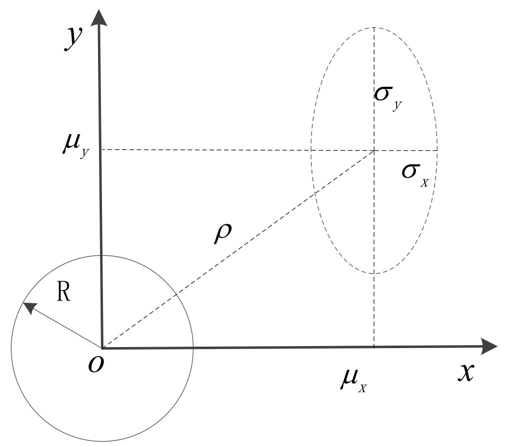

FIGURE 4. Integral calculation coordinate system.

$$\mathrm{Var}(e_{ef}) = \begin{bmatrix} \sigma_x^2 & 0 \\ 0 & \sigma_y^2 \end{bmatrix} \tag{10}$$

where σ_x, σ_y are the short semi axis and long semi axis of the ellipsoid, respectively, assuming $\sigma_x^2 \le \sigma_y^2$.

From the conclusion of the previous section, it can be seen that the position error of UAVs follows the Gaussian distribution in the encounter plane, and the probability density function is

$$f(x,y) = \frac{1}{2\pi\sigma_x\sigma_y} \exp\left[-\frac{1}{2}\left(\frac{(x-\mu_x)^2}{\sigma_x^2} + \frac{(y-\mu_y)^2}{\sigma_y^2}\right)\right] \tag{11}$$

Therefore, the probability of collision of two UAVs at time t is the integral of f(x, y) integral in the circle:

$$P_{xy} = \iint_{x^2+y^2 \le R^2} f(x,y)dxdy \tag{12}$$

where R is the sum of the envelope of the two UAVs, which is referred to as the joint envelope ball. The integral area of P_{xy} is the joint envelope ball area $x^2 + y^2 \le R^2$, which is swept by the error ellipsoid region V.

In this way, the problem of computing the collision probability in three-dimensional space is transformed into the integration of the density function in the two-dimensional circular domain, thus greatly reducing the computational complexity and the computing time. Fig. 4 shows the coordinate system used for integral calculation.

IV. ANALYSIS OF THE CALCULATION METHOD OF 4 COLLISION PROBABILITY

According to the analysis in chapter three, the problem of computing the collision probability is transformed into a two-dimensional integration of the density functions of the diagonal elements in the relative random error vector matrix inside the circle. To simplify the computation of the collision probability in two-dimensional space, a fast computation method based on compressed space and infinite series is proposed in this section to solve the problems of the probability integration being complex and the calculation time being long.

The integral region can be approximated from an elliptic domain to a circle domain

In formula (11), we assume that the relative variance of the random error vector e_{ef} matrix $Var(e_{ef})$ of two UAVs is a diagonal matrix in which $\sigma_x = \sigma_y = \sigma$. Then, the error ellipse's long axis and short half axis are equal, so that the error ellipse becomes a circle $x^2 + y^2 \le \sigma^2$. Using space compression, the probability density function in formula (12) can be changed into

$$f_{SC}(x', y') = \frac{1}{2\pi\sigma^2} \exp\left(-\frac{(x'-\mu'_x)^2 + (y'-\mu'_y)^2}{2\sigma^2}\right) \tag{13}$$

Normally, we can assume that $k = \frac{\sigma_x}{\sigma_y}$; thus,

$$P_{xy-\sigma} = \iint\limits_{\frac{x'^2}{a^2}+\frac{y'^2}{b^2}\le 1} f(x', y')dx'dy' \tag{14}$$

The long axis of the integral ellipse is $a = r_a$, and the short axis half shaft length is $b = kr_s$.

The elliptic integral region is approximated by a circular domain of equal size.

After the space compression of the above method, the integral region of the collision probability becomes the ellipse $E : \frac{x'^2}{a^2} + \frac{y'^2}{b^2} \le 1$. The area of this ellipse is $S_E = \pi ab = k\pi r_a^2$. To simplify the complexity of the integral region, E is equivalent to a circle C_E with the same area, the center of the circle coincides with the central position of the ellipse, and the radius is $R_C = \sqrt{ab} = \sqrt{k} r_a$, giving the equation of C_E as $x^2 + y^2 \le R_C^2$. Then, the integral value in the ellipse of equal variance can be equal to the integral value of equal area. Fig. 5 shows that replacing the ellipse field with a circle of equal area.

$$P_{xy-\sigma} \approx \frac{1}{2\pi\sigma^2} \iint\limits_{C_E} \exp\left[-\frac{(x'-\mu'_x)^2 + (y'-\mu'_y)^2}{2\sigma^2}\right]dx'dy' \qquad C_E : x'^2 + y'^2 \le R_C^2 \tag{15}$$

When $k = 1$, $R_C = R$ is the sum of the radii of the enveloping spheres of the two UAVs.

(2) The infinite series method is used to integrate the equal variance probability density function in the circle

① The double integral of the probability density function is divided into a heavy integral

The problem of the collision probability P_{xy} in the elliptic domain integral computation can be transformed into the integral of the equal variance probability density function in the circle domain:

$$P_{xy-\sigma} \approx \frac{1}{2\pi\sigma^2} \iint\limits_{C_E} f_{SC}(x', y')dx'dy' \quad C_E : x'^2 + y'^2 \le R_C^2 \tag{16}$$

In this section, to facilitate discussion, formula (16) is abbreviated form as $P = \iint\limits_{C} f(x,y)dxdy$, and

$$\begin{cases} f(x,y) = \dfrac{1}{2\pi\sigma^2} \exp\left[-\dfrac{(x-\mu_x)^2 + (y-\mu_y)^2}{2\sigma^2}\right] \\ x^2 + y^2 \le R^2 \end{cases} \tag{17}$$

Assuming that $\begin{cases} x = r\cos\theta \\ y = r\sin\theta, \end{cases}$ $\begin{cases} \mu_x = \rho\cos\theta_\rho \\ \mu_y = \rho\sin\theta_\rho, \end{cases}$ formula (16) can be changed into

$$P = \frac{1}{2\pi\sigma^2} \int_0^R r\exp(-\frac{r^2+\rho^2}{2\sigma^2}) \times \left[\int_0^{2\pi} \exp\left(\frac{r\rho\cos(\theta-\theta_\rho)}{\sigma^2}\right) d\theta\right] dr \tag{18}$$

Also, the integral formula of $\int_0^{2\pi} \exp\left(\frac{r\rho\cos(\theta-\theta_\rho)}{\sigma^2}\right) d\theta$ is $\exp\left(\frac{r\rho\cos(\theta-\theta_\rho)}{\sigma^2}\right)$, which can be written by the Taylor series as follows:

$$\exp\left(\frac{r\rho\cos(\theta-\theta_\rho)}{\sigma^2}\right) = \sum_{k=0}^{\infty} \frac{1}{k!} \frac{r^k\rho^k}{\sigma^{2k}} \cos^k(\theta-\theta_\rho) \tag{19}$$

The integral formula that is substituted by formula (18) is derived as follows:

$$\begin{aligned} &\int_0^{2\pi} \exp\left(\frac{r\rho\cos(\theta-\theta_\rho)}{\sigma^2}\right) d\theta \\ &= \int_0^{2\pi} \sum_{k=0}^{\infty} \frac{1}{k!} \frac{r^k\rho^k}{\sigma^{2k}} \cos^k(\theta-\theta_\rho)d\theta \\ &= \sum_{k=0}^{\infty} \frac{1}{k!} \frac{r^k\rho^k}{\sigma^{2k}} \int_0^{2\pi} \cos^k(\theta-\theta_\rho)d\theta \end{aligned} \tag{20}$$

By the integral principle of trigonometric function:

$$\int_0^{2\pi} cos^k\,(\theta-\mu_\theta)\,d\theta = \begin{cases} 2\pi\dfrac{(k-1)!!}{k!!} & k \textit{ is even} \\ 0 \quad k \textit{ is odd number} \end{cases} \tag{21}$$

Thus, formula (20) can be written in the following form:

$$\begin{aligned} &\sum_{k=0}^{\infty} \frac{1}{k!} \frac{r^k\rho^k}{\sigma^{2k}} \int_0^{2\pi} \cos^k(\theta-\theta_\rho)d\theta \\ &= 2\pi \sum_{m=0}^{\infty} \frac{1}{(2m)!} \frac{r^{2m}\rho^{2m}}{\sigma^{4m}} \frac{(2m-1)!!}{2m!!} \\ &= 2\pi \sum_{m=0}^{\infty} \frac{1}{(2m)!!(2m)!!} \frac{r^{2m}\rho^{2m}}{\sigma^{4m}} = 2\pi \sum_{m=0}^{\infty} \frac{1}{m!m!} \frac{r^{2m}\rho^{2m}}{2^{2m}\sigma^{4m}} \\ &= 2\pi \sum_{m=0}^{\infty} \frac{1}{m!m!} \left(\frac{r\rho}{2\sigma^2}\right)^{2m} \end{aligned} \tag{22}$$

where $\sum_{m=0}^{\infty} \frac{1}{m!m!} \left(\frac{r\rho}{2\sigma^2}\right)^{2m} = I_0(\frac{r\rho}{\sigma^2})$ and $I_0(x) = \sum_{k=0}^{\infty} \frac{1}{k!k!} \left(\frac{x}{2}\right)^{2k}$.

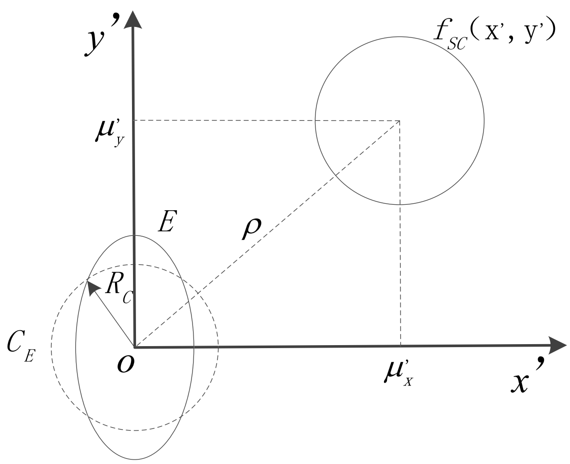

FIGURE 5. **Circle of equal area domain instead of the elliptical domain.**

Finally, the integral formula can be expressed as

$$\int_0^{2\pi} \exp\left(\frac{r\rho\cos(\theta-\theta_\rho)}{\sigma^2}\right)d\theta = 2\pi I_0\left(\frac{r\rho}{\sigma^2}\right) \tag{23}$$

Substituting formula (22) into formula (18) gives

$$P = \int_0^R \frac{r}{\sigma^2}\exp\left(-\frac{r^2+\rho^2}{2\sigma^2}\right) I_0\left(\frac{r\rho}{\sigma^2}\right)dr \tag{24}$$

According to (22), the expansion of $I_0\left(\frac{r\rho}{\sigma^2}\right)$ in formula (23) is shown in the following:

$$\begin{aligned} & I_0\left(\frac{r\rho}{\sigma^2}\right) \\ & = 1+\left(\frac{r\rho}{2\sigma^2}\right)^2+\frac{1}{4}\left(\frac{r\rho}{2\sigma^2}\right)^4+\ldots+\frac{1}{k!k!}\left(\frac{r\rho}{2\sigma^2}\right)^{2\mathrm{k}}+\ldots \\ & = I_0^{(0)}+I_0^{(1)}+I_0^{(2)}+\ldots+I_0^{(\mathrm{k})}+\ldots \end{aligned} \tag{25}$$

The probability density can be expressed as

$$\begin{aligned} P &= \int_0^R \frac{r}{\sigma^2}\exp\left(-\frac{r^2+\rho^2}{2\sigma^2}\right) \\ &\quad \times\left(I_0^{(0)}+I_0^{(1)}+I_0^{(2)}+\ldots+I_0^{(\mathrm{k})}+\ldots\right)dr \\ &= \sum_{\mathrm{k}=0}^{\infty}\int_0^R \frac{r}{\sigma^2}\exp\left(-\frac{r^2+\rho^2}{2\sigma^2}\right)I_0^{(\mathrm{k})}dr \end{aligned} \tag{26}$$

Let $\mathrm{P_k} = \int_0^R \frac{r}{\sigma^2}\exp\left(-\frac{r^2+\rho^2}{2\sigma^2}\right)I_0^{(\mathrm{k})}dr$; then,

$$P = P_0+P_1+P_2+P_3+\ldots+P_k+\ldots = \sum_{\mathrm{k}=0}^{\infty}P_k \tag{27}$$

Thus, the integral of the probability density function turns into the form of infinite series. Now, calculating P_0, we can obtain

$$P_0 = \int_0^R \frac{r}{\sigma^2}\exp\left(-\frac{r^2+\rho^2}{2\sigma^2}\right)dr = e^{-\frac{\rho^2}{2\sigma^2}}\left(1-e^{-\frac{R^2}{2\sigma^2}}\right) \tag{28}$$

Assume that $v = \frac{1}{2}\left(\frac{\rho}{\sigma}\right)^2$ and $u = \frac{1}{2}\left(\frac{R}{\sigma}\right)^2$; then,

$$P_0 = e^{-v}\left(1-e^{-u}\right) \tag{29}$$

Using the method of partial integration, we can compute term K of the infinite series P_{k}:

$$\begin{aligned} P_k &= \int_0^R \frac{r}{\sigma^2}\exp\left(-\frac{r^2+\rho^2}{2\sigma^2}\right)\frac{1}{k!k!}\left(\frac{r\rho}{2\sigma^2}\right)^{2\mathrm{k}}dr \\ &= \frac{\rho^2}{2k\sigma^2}P_{k-1}-\frac{1}{k!k!}\left(\frac{R\rho}{2\sigma^2}\right)^{2\mathrm{k}}\exp\left(-\frac{R^2+\rho^2}{2\sigma^2}\right) \\ &= \frac{v}{k}P_{k-1}-\frac{u^kv^k}{k!k!}e^{-(u+v)} \quad k\geq 1 \end{aligned} \tag{30}$$

Define $a_k = \frac{v}{k}$, $b_k = \frac{u^kv^k}{k!k!}e^{-(u+v)}$. Then, formula (30) can be expressed as follows:

$$P_k = a_kP_{k-1}-b_k \quad k\geq 1 \tag{31}$$

After the above calculation, the infinite series expression of the collision probability integral is $P_0 = e^{-v}\left(1-e^{-u}\right)$, and we can determine that the recurrence relation of the infinite series is formula (30). Thus, we can estimate any term $P_k(k\geq 1)$.

According to the infinite series method, we can take the sum of forward terms to approximate the result of the infinite series:

$$P \approx P_0+P_1+P_2+\cdots\cdots+P_n = \sum_{i=0}^{n}P_i \tag{32}$$

Assume that the truncation error of the set probability is P_{s} and that the value of P_{s} at this time is

$$P_s = P-\sum_{i=0}^{n}P_i \tag{33}$$

③ Analysis of the truncation error

From the analysis of the approximation error in ②, we can see the recurrence formula of the infinite series of probability integral, such as formula (30). Therefore, $\mathrm{P_k}$ can be expressed as

$$P_k = \left(\prod_{i=1}^{k}a_i\right)P_0-\sum_{j=1}^{k}\left(b_j\prod_{i=j+1}^{k}a_i\right) \tag{34}$$

Substituting formula (33) with the expressions of P_0, a_{k}, and b_{k}, we have

$$\begin{aligned} P_k &= \left(\prod_{i=1}^{k}a_i\right)P_0-\sum_{j=1}^{k}\left(b_j\prod_{i=j+1}^{k}a_i\right) \\ &= \frac{v^k}{k!}P_0-\sum_{j=1}^{k}\left(b_j\left(\prod_{i=j+1}^{k}a_i\right)\Big/\left(\prod_{i=1}^{j}a_i\right)\right) \\ &= \frac{v^k}{k!}e^{-(v+u)}\left(e^u-\sum_{j=0}^{k}\frac{u^j}{j!}\right) \end{aligned} \tag{35}$$

Therefore, the collision probability P is

$$P=\sum_{k=0}^{\infty}P_k=e^{-(u+v)}\sum_{k=0}^{\infty}\frac{v^k}{k!}\left(e^u-\sum_{j=0}^{k}\frac{u^j}{j!}\right) \tag{36}$$

e^u can be written with the Taylor series:

$$e^u=\sum_{j=0}^{k}\frac{u^j}{j!}+R_{k+1}(u)=\sum_{j=0}^{k}\frac{u^j}{j!}+\frac{u^{k+1}e^{\xi_k}}{(k+1)!}\quad(0<\xi_k<u) \tag{37}$$

Substituting formula (36) with formula (37) gives

$$P_k=\frac{u^{k+1}v^k}{k!(k+1)!}e^{-(v+u)}e^{\xi_k} \tag{38}$$

Then, the collision probability P is

$$P=e^{-(v+u)}\sum_{k=0}^{\infty}\frac{u^{k+1}v^k}{k!(k+1)!}e^{\xi_k} \tag{39}$$

Then, the upper bound of the truncation error P_s is

$$P_s<\frac{1}{n!(n+1)!}u^{n+1}v^n e^{-v}e^{uv} \tag{40}$$

By formula (40), we can determine that the size of the truncation error P_s has dimensionless variables u and v, which are the ratio of ρ and R and σ, respectively; n also affects the truncation error. Usually, the radius R_S of the UAV combined envelope is only a few meters or even smaller, and R has the same magnitude. Because $u=\frac{1}{2}\left(\frac{R}{\sigma}\right)^2$, the value of u will be very small. Regardless of how large the ratio of ρ to σ is, when the value of n is sufficiently large, the upper bound of the truncation error values will be very small. As shown in Table 1, when ρ, R and σ take different values, there is an upper limit value of P_s, whose standard units are km.

TABLE 1. Truncation error in the different cases.

	Case 1	Case 2	Case 3	Case 4
σ	0.05	2.0	1.732	2.0
ρ	0.01	1.5	1.0	10.0
R	0.005	0.01	0.01	0.01
$P\approx P_0$	0.00489	9.4354e-006	1.4109e-005	4.6583e-011
$P_s(n=1)$	2.4507e-007	1.6586e-011	1.9598e-011	3.6399e-015
$P_s(n=1)/P$	5.0130e-005	1.7578e-006	1.3891e-006	7.8138e-005
$P\approx P_0+P_1$	0.00489	9.4355e-006	1.4109e-005	4.6587e-011
$P_s(n=2)$	4.0846e-012	9.7183e-018	9.0741e-018	9.4789e-020
$P_s(n=2)/P$	8.3546e-010	1.0300e-012	6.4316e-013	2.0347e-009

From the analysis of Table 1, we can see that when the infinite series is used as the integral value of the collision probability, the relative error between the truncation error and the probability value at this time is $P_s(n=1)/P$, and its magnitude is 10^{-5} or perhaps smaller. When using the first two points of the infinite series as the collision probability value, the relative error between the truncation error and the probability value is $P_s(n=2)/P$, which has a magnitude of 10^{-9}. Therefore, we can draw the following conclusions: this approximation method can be used for UAV collision, and its probability calculation is small and easy to achieve with high precision and low complexity. Therefore, the collision probability is shown as follows:

$$P_{xy}=e^{-v}\left(1-e^{-u}\right) \tag{41}$$

After analyzing the deduction process of the above compressed space and approximate integral region, we can see that the upper form can be written as follows:

$$P_{xy}=\exp\left[-\frac{1}{2}\left(\frac{\mu_x^2}{\sigma_x^2}+\frac{\mu_y^2}{\sigma_y^2}\right)\right]\left[1-\exp\left(-\frac{r_a^2}{2\sigma_x\sigma_y}\right)\right] \tag{42}$$

V. EXPERIMENTAL SIMULATION BASED ON THE BASIC KALMAN FILTERING ALGORITHM

A. TYPES OF GRAPHICS

As shown in Figure 6, the system model is defined as

$$X_k=\Phi X_{k-1}+\Gamma u_k+v\quad \textit{State Equation}$$
$$Y_k=CX_{k-1}+w\quad \textit{Observation equation}$$

Given the input *u(t)=sin(t)*, R and Q are the covariance for v and w, respectively, and both have values of 1. In Figure 6, the upper figure compares the true trajectory (dashed line) and the trajectory (solid line) processed by the Kalman filter. The lower figure compares the observation noise (dashed line) and the estimated noise (solid line). From the diagram, we can see that the Kalman filter can greatly limit the interference and influence of noise.

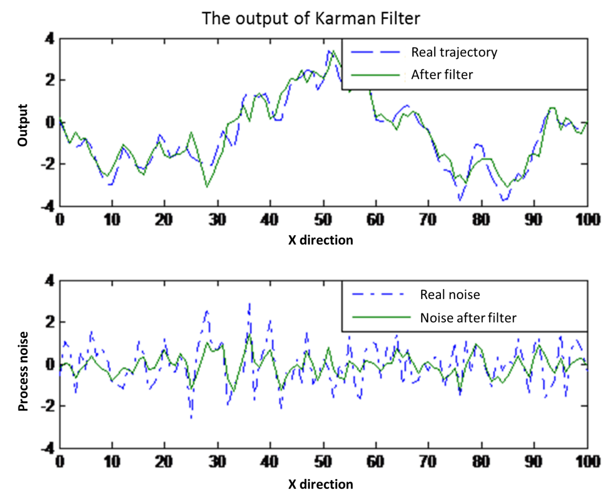

FIGURE 6. A complete picture of the operation of the Kalman filter.

In the simulation experiment, the simulation area is established in the two-dimensional plane, and the area of the plane is 100 km*100 km. There are thirteen obstacles, the radius of the safety envelope ball of the obstacle r_3 is 5 km, and the safety warning radius r_2 is 3 km. The UAVs have a fixed speed of 100 m/s, and the maximum turning angle is 60 degrees. Simulation experiments are carried out under different conditions. The starting point coordinates of the three formation UAV are (0,18), (0,50) and (0,85). The coordinates of the targets are (100,18), (100,50) and (100,85). In this experiment, if the distance between the UAVs is less than r2+r3, then the track of the UAV will be affected.

To facilitate comparison of the experimental results, UAV-C does not add any noise or Kalman prediction algorithm. The ideal flight path of three groups of UAVs in the noiseless condition is shown in Figure 7.

For the case of zero communication noise, Fig. 7 shows the ideal path planning of the three UAV formation teams. To verify the effectiveness of the proposed algorithm, we add Gaussian white noise, which is shown in Fig. 8.

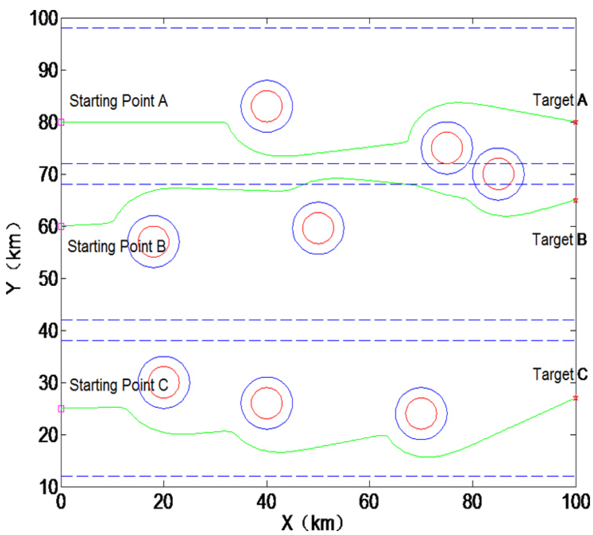

FIGURE 7. UAV path planning based on artificial potential field hierarchical flight of the UAV route planning model (ideal flight model).

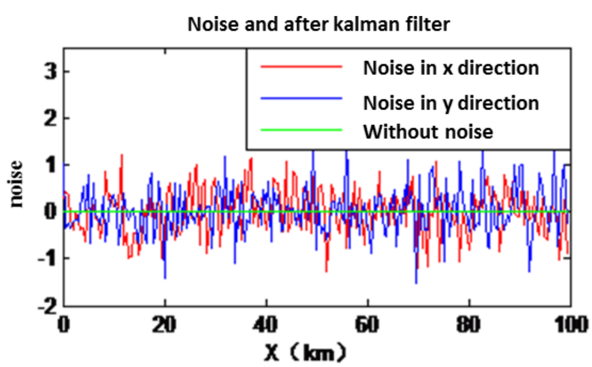

FIGURE 8. Resulting deviation from the noise of the state of information and communication.

Fig. 9 shows the track and collision probabilities of formation flying UAV group at 0.2 times the communication noise interference. Figure 9 (a) shows the tracks of UAV-A

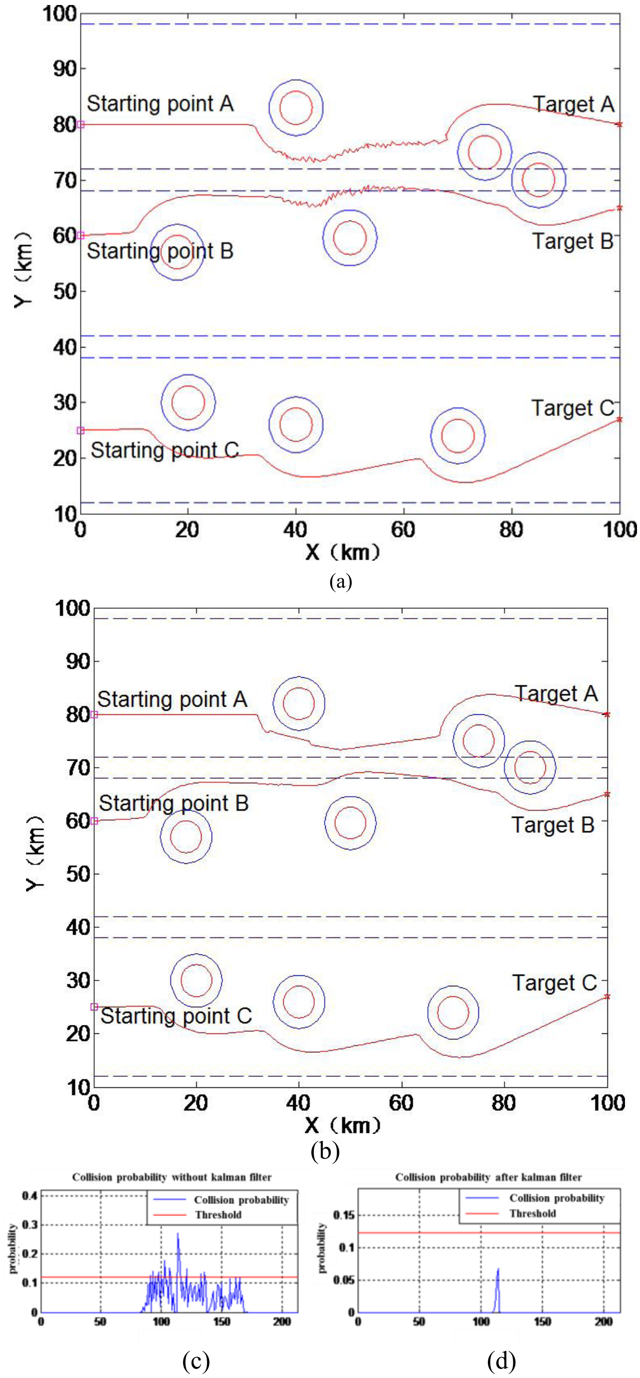

FIGURE 9. Formation UAV-A track and probability of UAV-B group at 0.2 times the noise value.

and UAV-B in the formation UAV group at 0.2 times the noise. Tt can be seen from this figure that when the distance between the two groups D_k is longer than $r_2 + r_3$, each track will not change because changing the noise state impacts the UAV flight. When the distance between the two UAVs D_k is less than or equal to $r_2 + r_3$, each track will fluctuate. Fig. 9 (b) is the track processed by the Kalman state estimation algorithm, in which the sampling period Δt is 1 s and the filter's parameters are $P = 1$, $S = 0$, and $R = 1$; Fig. 9 (b) is obviously smooth. Fig. 9 (c) is the collision probability of UAV-A and UAV-B corresponding to Fig. 9 (a), and the collision probability of UAV-A and UAV-B corresponding to Fig. 9 (b) is shown in Figure 9 (d). The collision probability shows that with the communication noise of 0.2 times, the collision possibility of UAV-A and UAV-B is relatively large without Kalman treatment; however, the track after Kalman treatment is smoother, and the collision probability is greatly reduced. The comparison results show that the Kalman state estimation algorithm can effectively reduce the collision probability of the aircraft when the communication is affected by 0.2 times the Gaussian white noise.

VI. CONCLUSION

In this paper, the method for calculating the collision probability of UAVs is introduced. Based on the communication noise, the state prediction is carried out using the Kalman filter. The simulation experiment shows that the probability calculation is a good way to prove the control strategy.

REFERENCES

[1] S. D. Bopardikar, B. Englot, and A. Speranzon, "Multiobjective path planning: Localization constraints and collision probability," *IEEE Trans. Robot.*, vol. 31, no. 3, pp. 562–577, Jun. 2015.
[2] Y.-L. Chen, "A forward collision probability index based on the driving behavior," in *Proc. IEEE 84th Veh. Technol. Conf.*, Sep. 2016, pp. 1–5.
[3] J. Park and J. Kim, "Predictive evaluation of ship collision risk using the concept of probability flow," *IEEE J. Ocean. Eng.*, vol. 42, no. 4, pp. 836–845, Oct. 2017.
[4] Y. Akagi and P. Raksincharoensak, "Longitudinal and lateral motion planning method for avoidance of multi-obstacles in urban environments based on inverse collision probability," in *Proc. IEEE Intell. Veh. Symp.*, Jun. 2016, pp. 827–832.
[5] Y. L. Chen, "An explicit and novel forward collision probability index," in *Proc. IEEE 10th Conf. Ind. Electron. Appl.*, Jun. 2015, pp. 1778–1782.
[6] J. L. Foster and H. S. Estes, "A parametric analysis of orbital debris collision probability and maneuver rate for space vehicles," NASA Johnson Space Flight Center, Houston, TX, USA, Tech. Rep. NASA/JSC-25898, 1992.
[7] P. R. Patera, "General method for calculating satellite collision probability," *J. Guid., Control, Dyn.*, vol. 24, no. 4, pp. 716–722, 2001.
[8] R. P. Patera, "Quick method to determine long-term orbital collision risk," in *Proc. AIAA Satmax Conf.*, 2002, Art. no. AIAA-2002-1809.
[9] R. P. Patera, "Conventional form of the collision probability integral for arbitrary space vehicle shape," in *Proc. AIAA/AAS Astrodyn. Specialist Conf. Exhibit*, Providence, RI, USA, 2004, p. 5218.
[10] R. P. Patera, "Calculating collision probability for arbitrary space vehicle shapes via numerical quadrature," *J. Guid., Control, Dyn.*, vol. 28, no. 6, pp. 1326–1328, 2005.
[11] S. Alfano, "Accommodating rectangular objects in probability calculations," in *Proc. AIAA/AAS Astrodyn. Specialist Conf. Exhibit*, Providence, RI, USA, 2004, p. 5217.
[12] S. Alfano, "A numerical implementation of spherical object collision probability," *J. Astron. Sci.*, vol. 53, no. 1, pp. 103–109, 2005.
[13] S. Alfano, "Satellite collision probability enhancements," *J. Guid., Control Dyn.*, vol. 29, no. 3, pp. 588–592, 2006.
[14] S. Alfano, "Beta conjunction analysis tool," in *Proc. AAS/AIAA Space Flight Mechan. Meeting*, 2007, p. 393.
[15] F. K. Chan, *Spacecraft Collision Probability*. El Segundo, CA, USA: Aerospace Press, 2008.
[16] F. K. Chan, "Collision probability analyses for Earth-orbiting satellites," *Adv. Astron. Sci.*, vol. 96, pp. 1033–1048, 1997.
[17] F. K. Chan, "Analytical expressions for computing spacecraft collision probabilities," in *Proc. AAS/AIAA Space Flight Mech. Meeting*, Santa Barbara, CA, USA, 2001, pp. 305–320.
[18] F. K. Chan, "Improved analytical expressions for computing spacecraft collision probabilities," in *Proc. AAS/AIAA Space Flight Mech. Meeting*, 2003, p. 184.
[19] S. Alfano, "Review of conjunction probability methods for short-term encounters," in *Proc. AAS/AIAA Space Flight Mech. Meeting*, 2007, p. 148.
[20] *Draft Recommendation for Space Data System Standards: Conjunction Data Message*. document Draft recommended standard CCSDS 508.0-R-1, CCSDS Secretariat, 2012.
[21] R. Zeng, W. Sheng, and D. Yang, "Collision probability computation based on vehicle to vehicle communication," in *Proc. IEEE Int. Conf. Cyber Technol. Autom. Control, Intell. Syst.*, Jun. 2015, pp. 1462–1467.

ZHENYU WU received the Ph.D. degree from the Dalian University of Technology in 2014. His research interests include intelligent control, robotics, and embedded applications.

JINHUAN LI received the B.S. degree from the Dalian University of Technology in 2014, where he is currently pursuing the M.S. degree. His research interests include path planning and signal processing.

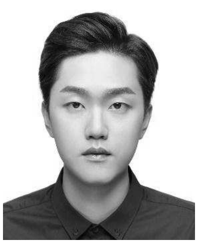

JIAMING ZUO is currently pursuing the B.S. degree with the Dalian University of Technology. His research interest includes robot control.

SHENGMING LI received the M.S. degree from the Dalian University of Technology in 2014, where he is currently pursuing the Ph.D. degree. His research interests include robot control and data processing.